Evolution of Pore Volume Distribution During Gasification

A general equation is derived that predicts the evolution of pore volume distribution during isothermal gasification in the regime of kinetic control, starting from a given initial condition. The development takes into account pore enlargement as well as pore intersections. Equations are also derived for the special cases of (1) uniform pore size and (2) bimodal distribution. The results are used to interpret the experimental data of Tomkow et al. (1977) and Kawahata and Walker (1962).

JOW-LIH SU and D. D. PERLMUTTER

Department of Chemical Engineering
University of Pennsylvania
Philadelphia, PA 19104

SCOPE

When a gasification reaction occurs within a porous solid the pore structure of the reacting solid changes with conversion. Such changes are especially important for the production of a solid product (e.g., activated carbon) whose adsorption performance is closely associated with the pore structure that is developed. To quantify such changes, a general equation is derived that predicts the evolution of pore volume distribution during gasification from a given initial condition. This development is an extension of the previous random pore model (Bhatia and Perlmutter, 1980; Gavalas, 1980) for isothermal reaction in the regime of kinetic control. It considers pore enlargement as well as the effects of pore intersections.

CONCLUSIONS AND SIGNIFICANCE

A general equation is derived that predicts the evolution of pore volume distribution during gasification from a given initial condition. The special cases of uniform pore size and bimodal distribution are also considered. As reaction proceeds the pore volume first increases, the smaller pores growing faster because of the larger surface to volume ratio. However, at higher conversions the pore volume increase due to pore growth is reduced by pore intersections, resulting eventually in net decreases in surface area and pore volume in particular pore size ranges. This development provides the background that can be useful for designing or tailoring the pore structure of activated carbons for specific uses.

For solids with uniform pore size, the results closely follow those predicted by the Petersen (1957) model over a range of conversions. For solids with a bimodal pore volume distribution, the evolution of large and small pore volumes occurs at different relative rates, producing a minimum ratio of volumes at a specific converison level. The results of this study are applied to interpret the experimental data reported by Tomkow et al. (1977) and Kawahata and Walker (1962).

INTRODUCTION

One distinctive feature of a char gasification reaction is the change in pore structure of the solid reactant that occurs continuously as reaction proceeds. This evolution of pore structure affects not only the gasification kinetics (Dutta et al., 1977; Dutta and Wen, 1977), but also the properties of the unreacted residue, notably its adsorption capabilities (Hashimoto et al., 1979) and resistance to gas diffusion (Patel et al., 1972; Walker, 1980). Such changes are of special importance in the production of activated carbons whose adsorption performance is closely related to their pore structure, and many experimental studies (Cameron and Stacy, 1958; Cameron and Stacy, 1959; Kawahata and Walker, 1962; Tomkow et al., 1977; Hashimoto et al., 1979) have been devoted to measurement of changes during gasification with the ultimate objective of obtaining suitable pore structures for specific uses.

The pore structure of such a material is usually characterized by its pore volume distribution, obtained experimentally by mercury porosimetry and adsorption-desorption methods. Other integral properties of the pore structure, such as total surface area and total pore volume, can also be obtained directly from BET adsorption techniques and mercury-helium densities measurements; however, the pore volume distribution represents the most detailed pore structure information from which all the integral properties can be derived.

The characterization of the pore volume distribution is also critical in carbonaceous materials that possess pore structures similar to molecular sieves, for a slight enlargement of pore size by gasification can result in a drastic increase in adsorption capacity for particular adsorbates (Lamond and Marsh, 1964), even though the increase of total surface area and total pore volume are not otherwise significant.

Among proposals to model pore structure *during gasification*, one of the early models was by Petersen (1957), who assumed the solid to be comprised of cylindrical pores of uniform size. Using Petersen's formulation, Szekely et al. (1976) have derived equations that predict conversion in terms of the development of pore radius as

$$X = \frac{\epsilon_0}{1-\epsilon_0}\left[\left(\frac{r}{r_0}\right)^2 \frac{G-(r/r_0)}{G-1} - 1\right] \tag{1}$$

where G is the solution to the cubic equation

$$\frac{4}{27}\epsilon_0 G^3 - G + 1 = 0 \tag{2}$$

Later models have attempted to incorporate pore volume distributions. Hashimoto and Silveston (1973) adopted a population

balance technique to analyze the evolution of pore volume distribution with consideration of pore intersections. The results were expressed as a set of integral equations containing several parameters to be estimated from the experimental results. As a consequence, the model does not lend itself to a priori prediction of the evolution of pore structure. A pore-tree model was proposed by Simons and Finson (1979) and Simons (1979), also requiring several empirical relations on the pore structure.

As reaction proceeds the pore volume first increases as pore size is enlarged by reaction. However, at higher conversions the pore volume increase due to pore growth is reduced by pore intersections, resulting eventually in net decreases in total surface area and pore volume in particular pore size ranges. Bhatia and Perlmutter (1980) and independently Gavalas (1980) have shown that if the pore overlap is taken into account the evolution of surface area can be obtained in terms of overall conversion as:

$$\frac{S}{S_0} = (1 - X)\sqrt{1 - \psi \ln(1 - X)} \tag{3}$$

and the conversion dependence on time as

$$X = 1 - \exp\left[-k_s R t S_{E0}\left(1 + \psi \frac{k_s R t S_{E0}}{4}\right)\right] \tag{4}$$

with initial pore structure parameters ψ defined as

$$\psi = \frac{4\pi L_{E0}}{S_{E0}^2} \tag{5}$$

This model allows an arbitrary initial pore volume distribution within the solid, but does not explicitly predict its evolution. In the analysis that follows, the random pore model is extended to predict the development during gasification of the pore volume distributuion from a given initial condition.

MODEL DEVELOPMENT

Consider the isothermal gasification reaction of a particle of porous solid B with a fluid A according to

$$aA(g) + bB(s) \rightarrow pP(g) \tag{6}$$

If the diffusional resistances are all negligible, the reaction will take place uniformly on all the pore surfaces. As reaction progresses, reactant B will be depleted and each pore will grow in radius at the rate

$$\frac{dr}{dt} = k_s R(C) \tag{7}$$

For a pore with initial radius r_0, Eq. 7 integrates to

$$r = r_0 + k_s R t \tag{8}$$

Neighboring pores will ultimately intersect as the solid B separating them is consumed by reaction.

The actual pore volume of solid reactant B at any time may be considered to be the net result of the random overlapping of a set of cylinders of length distribution $f(r)$. If the cylinders did not overlap, $f(r)dr$ would be their total length per unit volume of space having radii between r and $r + dr$. The actual total pore length is less than the length of the hypothetical noninteracting cylinders because of the pore intersections and overlaps.

Pore Volume Distribution

The pore volume distribution function of a hypothetical nonoverlapped pore system can be defined by:

$$v_E(r,t) = \pi r^2 f(r,t) \tag{9}$$

with $v_E(r,0)$ as its initial distribution, and

$$L_E = \int_0^\infty f(r,t)dr \tag{10}$$

$$S_E = 2\pi \int_0^\infty r f(r,t)dr = 2\int_0^\infty \frac{v_E(r,t)}{r}dr \tag{11}$$

and

$$V_E = \pi \int_0^\infty r^2 f(r,t)dr = \int_0^\infty v_E(r,t)dr \tag{12}$$

as the total length, total surface, and total enclosed volume, respectively, of the hypothetical nonoverlapped cylindrical system.

As reaction proceeds, non-intersection pores initially having radius r_0 and total length $f(r_0,0)$ will become pores with radius $(r_0 + k_s R t)$ and with the same length. Therefore

$$f(r_0 + k_s R t, t) = f(r_0,0) \tag{13}$$

Consequently,

$$L_E = \int_0^\infty f(r,t)dr = \int_0^\infty f(r,0)dr = L_{E0} \tag{14}$$

The evolving pore volume distribution follows Eqs. 8, 9 and 13 in combination to give

$$v_E(r,t) = \pi(r_0 + k_s R t)^2 f(r,t)$$
$$= \pi r_0^2\left(1 + \frac{k_s R t}{r_0}\right)^2 f(r_0,0) \tag{15}$$

with the initial distribution

$$v_E(r_0,0) = \pi r_0^2 f(r_0,0) \tag{16}$$

Combining Eqs. 15 and 16 gives

$$v_E(r,t) = \left(1 + \frac{k_s R t}{r_0}\right)^2 v_E(r_0,0) \tag{17}$$

which describes the evolution of pore volume distributiuon of the nonoverlapped system. It remains to relate this distribution to the corresponding pore volume distribution of the actual system $v(r,t)$. To this end, Gavalas (1980) has shown in a slightly different context that on the average the volume enclosed by the actual (or overlapped) system is only a fraction of the volume enclosed by the nonoverlapped cylindrical system:

$$\int_r^\infty v(r',t)dr' = 1 - \exp\left[-\int_r^\infty v_E(r',t)dr'\right] \tag{18}$$

Taking the lower integration limit of Eq. 18 to be $r = 0$ gives a well-known relation derived earlier by Avrami (1940) from a different perspective and without the limitation of pore shape:

$$V = 1 - \exp(-V_E) \tag{19}$$

with initial condition:

$$V_0 = 1 - \exp(-V_{E0}) \tag{20}$$

where

$$V = \int_0^\infty v(r',t)dr' \tag{21}$$

Differentiation of Eq. 18 with respect to r yields

$$v(r,t) = v_E(r,t)\exp\left[-\int_r^\infty v_E(r',t)dr'\right] \tag{22}$$

or

$$v_E(r,t) = \frac{v(r,t)}{1 - \int_r^\infty v(r',t)dr'} \tag{23}$$

which describe the relationship of pore volume distribution function between overlapped and nonoverlapped systems.

Structure of Uniform Pore Size

The simplest pore structure exists in a solid if all the pores have the same radius. In this case, Eqs. 9 and 16 reduce to:

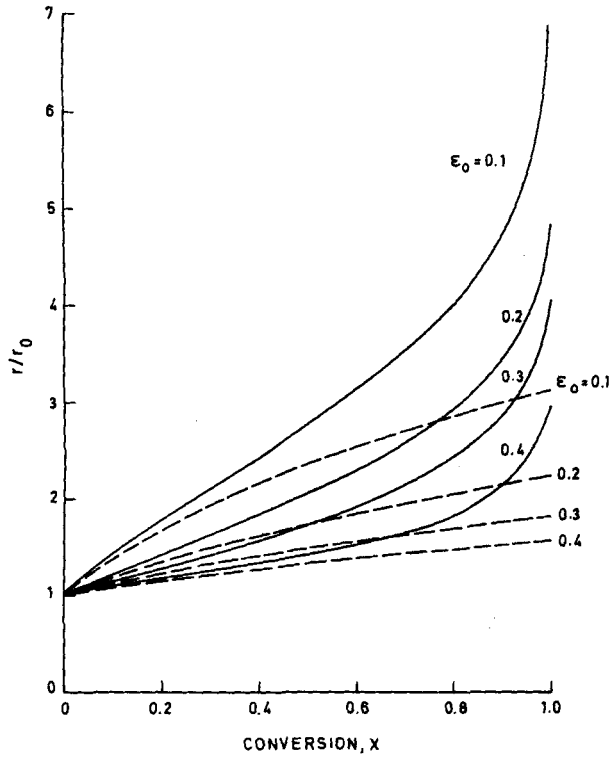

Figure 1. Effect of conversion on uniform pore size. Predictions of random pore model and nonoverlapped pore model are solid and dashed lines, respectively.

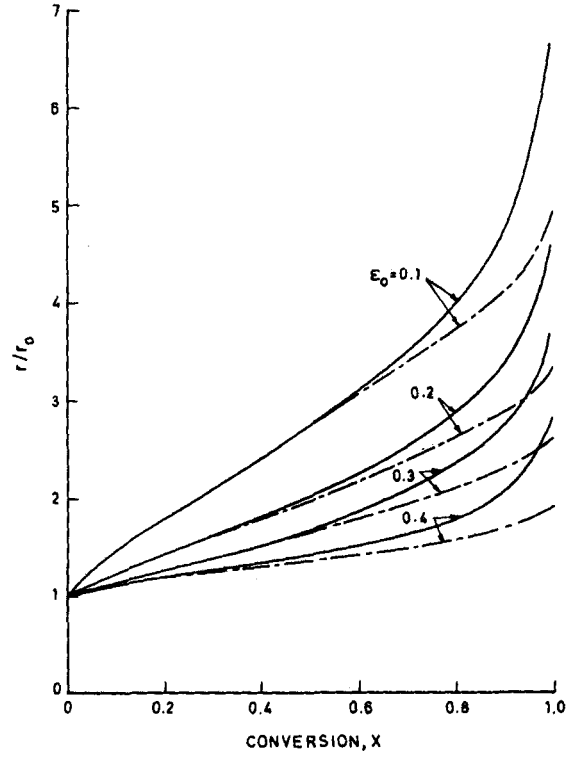

Figure 2. Effect of conversion on uniform pore size. Predictions of random pore model and Petersen (1957) model are solid and dashed lines, respectively.

$$V_E(t) = \pi r^2 L_E \tag{24}$$

and

$$V_{E0} = \pi r_0^2 L_{E0} \tag{25}$$

Combining these relations with Eqs. 14, 19 and 20 leads to:

$$\frac{1-V}{1-V_0} = \exp\{V_{E0} - V_E\}$$
$$= \exp\left\{-V_{E0}\left[\left(\frac{r}{r_0}\right)^2 - 1\right]\right\}$$
$$= [1-V_0]^{(r/r_0)^2-1} \tag{26}$$

Total pore volume can be related to the fractional conversion of solid B by

$$X = 1 - \frac{1-V}{1-V_0} \tag{27}$$

Therefore, Eq. 26 may also be written as

$$\frac{r}{r_0} = \sqrt{1 + \frac{ln(1-X)}{ln(1-\epsilon_0)}} \tag{28}$$

with pore volume equal to

$$V = 1 - (1-\epsilon_0)(1-X) \tag{29}$$

where $\epsilon_0 = v_0$ is the initial porosity.

This result is shown in Figure 1 in a form that lends itself to comparison with the case of nonintersecting pores, for which

$$\frac{r}{r_0} = \sqrt{\frac{V_E}{V_{E0}}} = \sqrt{\frac{V}{V_0}} = \sqrt{\frac{1-(1-\epsilon_0)(1-X)}{\epsilon_0}} \tag{30}$$

With small initial porosity ($\epsilon_0 = 0.1$) the effect of pore intersection is not significant in the early stages of reaction: the (r/r_0) results differ by less than 12% at $X < 0.20$. The differences do become larger, however, at the higher conversion levels for all values of initial porosity, and because of significant intersections considerably larger pore enlargement is needed to obtain the same increment of conversion.

Petersen (1957) also analyzed the evolution of pore size for a solid comprised of pores of a single size, and the result predicted by Eqs. 1 and 2 are shown for comparison in Figure 2. The results of Petersen's model follow closely the prediction of Eq. 28 except at conversionx $X \geq 0.60$. The deviations are to be expected, for while the Petersen model allows intersections, it does not attempt to account for the collapse of reaction surface by overlap.

Bimodal Pore Size Distribution

For the simplest bimodal distribution the solid reactant may be considered to contain initially pore volumes V_{10} and V_{20} located in narrow ranges centering about pore sizes r_{10} and r_{20}, respectively, with $r_{20} > r_{10}$. Following Eq. 22 one obtains

$$V_2 = V_{2E} \exp\left[-\frac{V_{2E}}{2}\right] \tag{31}$$

and

$$V_1 = V_{1E} \exp\left[-\left(\frac{V_{1E}}{2} + V_{2E}\right)\right] \tag{32}$$

where it is to be noted that the volumes V_1 and V_2 are approximated as also being located at specific r_1 and r_2, although they in fact cover a narrow range of pore sizes. Dividing Eq. 31 by Eq. 32:

$$\frac{V_2}{V_1} = \frac{V_{2E}}{V_{1E}} \exp\left[\frac{1}{2}(V_{1E} + V_{2E})\right] \tag{33}$$

Since $(V_{1E} + V_{2E}) = V_E = -ln(1-V)$, Eq. 33 reduces to:

$$\frac{V_2}{V_1} = \frac{V_{2E}}{V_{1E}} \frac{1}{\sqrt{1-V}} \tag{34}$$

By using Eq. 27 this relationship can also be expressed in terms of conversion as

$$\frac{V_2}{V_1} = \frac{V_{2E}}{V_{1E}} \frac{1}{\sqrt{(1-\epsilon_0)(1-X)}} \tag{35}$$

with initial condition

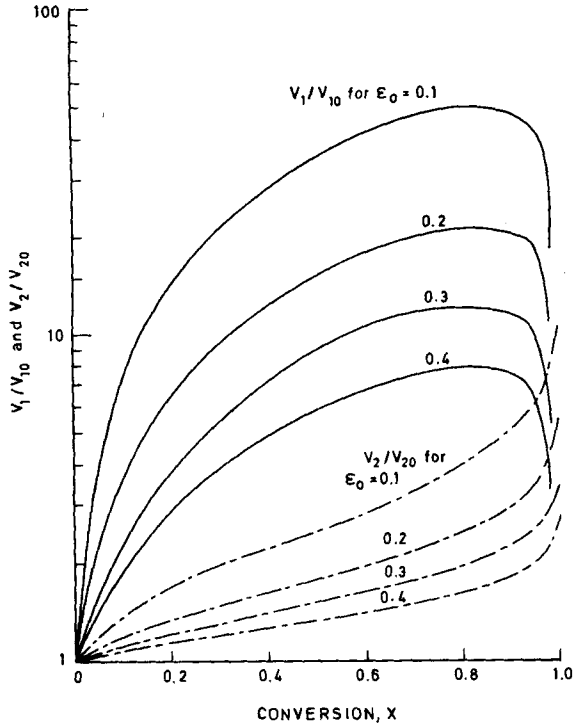

Figure 3. Effect of conversion on large and small pore volumes for a solid with bimodal pore size distribution. Large and small pore volumes are represented by solid and dashed lines, respectively.

$$\frac{V_{20}}{V_{10}} = \frac{V_{2E0}}{V_{1E0}} \frac{1}{\sqrt{1-\epsilon_0}} \tag{36}$$

By dividing Eq. 35 by Eq. 36 and substituting from Eq. 17 one can obtain

$$\frac{V_2}{V_1} = \frac{V_{20}}{V_{10}} \left[\frac{1 + \dfrac{k_s R t}{r_{20}}}{1 + \dfrac{k_s R t}{r_{10}}} \right]^2 \frac{1}{\sqrt{1-X}} \tag{37}$$

which together with

$$V_1 + V_2 = V = 1 - (1-\epsilon_0)(1-X) \tag{38}$$

allows one to calculate the evolution of pore volumes V_1 and V_2 with respect to conversion or reaction time from the given initial pore structure V_{10}, V_{20}, r_{10}, r_{20}. The reaction time can be related to conversion by Eq. 4.

The primary interest in a bimodal distribution attaches to the relative volume changes of the two size groups as converison increases. Typical results are shown in Figure 3, computed for a range of initial porosities from Eqs. 37, 38 and 4, and for a choice of $(r_{20}/r_{10}) = (V_{20}/V_{10}) = 10$. In general, small pore volume increases much faster than large pore volume at the early stages of conversion. This trend is reversed at the higher range of conversions when the small pore volume increased by further reaction is greatly reduced by intersection. It is noteworthy that at 80% or higher conversion levels the small pore volume can actually decline even though large pore volume continues increasing. This is emphasized in Figure 4: the ratio of pore volumes decreases sharply during the first 30% of conversion, as small pores outgrow large pores, and remains relatively flat between 30 and 70% conversion where pore volumes of both sizes increase at similar rates. After 70% conversion the ratio starts increasing again as small pore volume is lost by intersections. Tested by various V_{20}/V_{10} and r_{20}/r_{10} values, these trends are generally valid regardless of the initial pore structure. For comparison and possible use in designing structures of specific character, the evolution of corresponding surface area is also shown in Figure 4, obtained from Eq. 3.

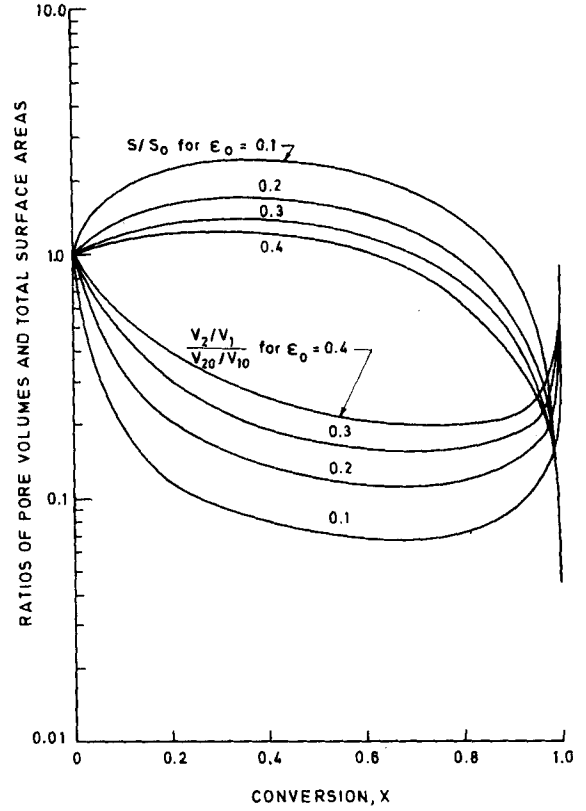

Figure 4. Effect of conversion on the ratios of pore volumes and total surface areas in a solid with bimodal pore size distribution.

Generalized Distribution

In order to generalize the treatment of evolving porosity to an arbitrary initial distribution, it is necessary to return to Eqs. 17 and 22. Combining these gives

$$v(r_0 + k_s R t, t) = \left(1 + \frac{k_s R t}{r_0}\right)^2 v_E(r_0,0) \times \exp\left[- \int_{r_0 + k_s R t}^{\infty} \left(1 + \frac{k_s R t}{r'}\right)^2 v_E(r',0)\, dr' \right] \tag{39}$$

where $v_E(r_0,0)$ can be related to the experimentally measured initial pore volume distribution $v(r_0,0)$ by Eq. 23. Replacing r_0 by the general variable r gives

$$v(r + k_s R t, t) = \frac{\left(1 + \dfrac{k_s R t}{r}\right)^2 v(r,0)}{1 - \displaystyle\int_r^{\infty} v(r',0)\, dr'} \times \exp\left[- \int_{r + k_s R t}^{\infty} \frac{\left(1 + \dfrac{k_s R t}{r'}\right)^2 v(r',0)}{1 - \displaystyle\int_{r'}^{\infty} v(r'',0)\, dr''} dr' \right] \tag{40}$$

When the initial porosity is small

$$v_E(r,0) \cong v(r,0) \tag{41}$$

and Eq. 40 can be simplified to

$$v(r + k_s R t, t) = \left(1 + \frac{k_s R t}{r}\right)^2 v(r,0) \times \exp\left[- \int_{r + k_s R t}^{\infty} \left(1 + \frac{k_s R t}{r'}\right)^2 v(r',0)\, dr' \right] \tag{42}$$

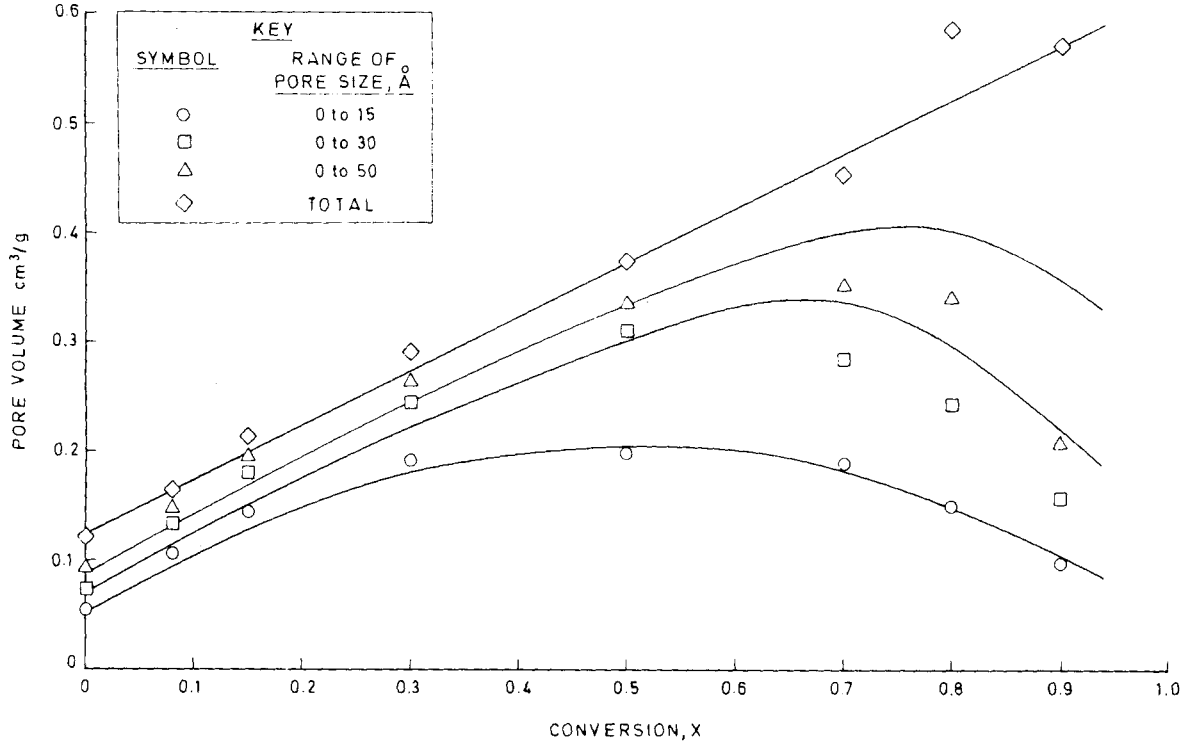

Figure 5. Comparison of model predictions on the evolution of pore volume distribution to the experimental data of Tomkow et al. (1977).

Equation 40 predicts the evolution of pore volume distribution of an actual pore system at any reaction time t from the given initial distribution $v(r,0)$. The combination of Eqs. 40 and 4 allows one to calculate the evolution of pore volume distribution with respect to the extent of reaction.

DATA INTERPRETATION AND DISCUSSION

Experimental data obtained by Tomkow et al. (1977) may be used to test Eq. 40 as a model for the evolution of pore volume distribution. By measuring benzene vapor adsorption at 298 K, these authors determined pore volumes at different levels of burn-off (conversion) as they oxidized a semi-coke previously generated by heating a xylitic brown coal under argon at 773 K. Cumulative pore volumes were reported for five ranges of pore radius: less than 15 Å, 15 to 30 Å, 30 to 50 Å, 50 to 100 Å, and 100 to 1,000 Å. The initial total pore volume of the semicoke before oxidation was 0.12 cm^3/g and the total pore volume at 90% burn-off was 0.57 cm^3/g. The initial porosity can therefore be calculated as 0.194, even though not given explicitly. To establish a continuous initial pore volume distribution, the reported cumulative pore volumes within each range of pore size were evenly subdivided to cover the entire size range. The increment of pore size chosen for computation was 3 Å from 0 to 30 Å, and 5 Å from 30 to 50 Å. For pores larger than 50 Å, the pore volume was assumed to be contributed completely by pores with radius of 55 Å.

Having established the initial distribution and porosity, the ensuing evolution of pore volume distribution with respect to conversion can be calculated from Eqs. 40 and 4. The computed results are shown in Figure 5 and compared with the reported experimental data. The agreement is remarkable in view of the uncertainties that are usually incorporated in the experimental technique for measuring pore volume distribution. The pore volume within the range of 0 to 15 Å reached a maximum at 50% burn-off. Since most of the surface area is contained in this micropore region the total surface area measured by Tomkow et al. (1977) also showed a maximum at 50%.

Another source of test data may be found in the work of Kawahata and Walker (1962), who conducted an extensive study of the pore structures of an Anthracite char during its reactions with CO_2 at temperatures between 800 and 950°C. In contrast to the samples studied by Tomkow et al. (1977), the Anthracite char contains mainly pores smaller than 30 Å diameter, which account for more than 92% of the total pore volume. The pore structure of this char can therefore be approximated as having a single pore size. The authors reported the evolution of average pore diameter at different levels of burn-off under various reaction conditions. As shown in Figure 6, the experimental data closely follow the pre-

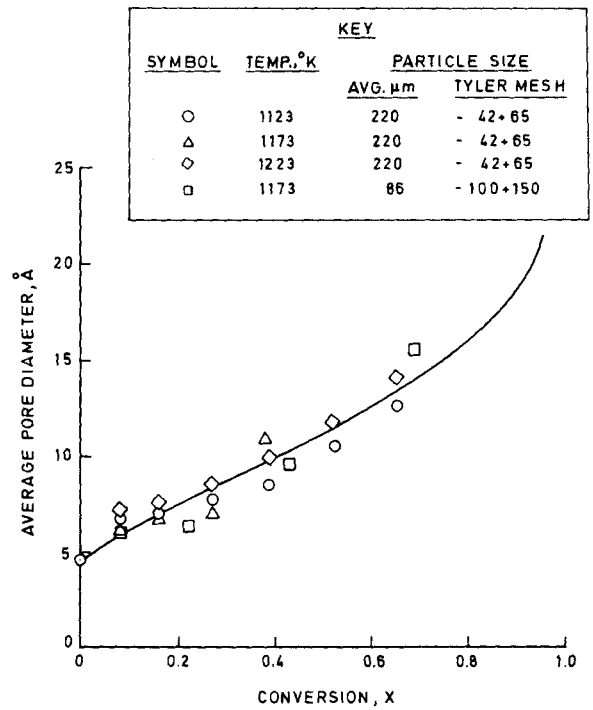

Figure 6. Comparison of model predictions on the change of pore size to the experimental data of Kawahata and Walker (1962).

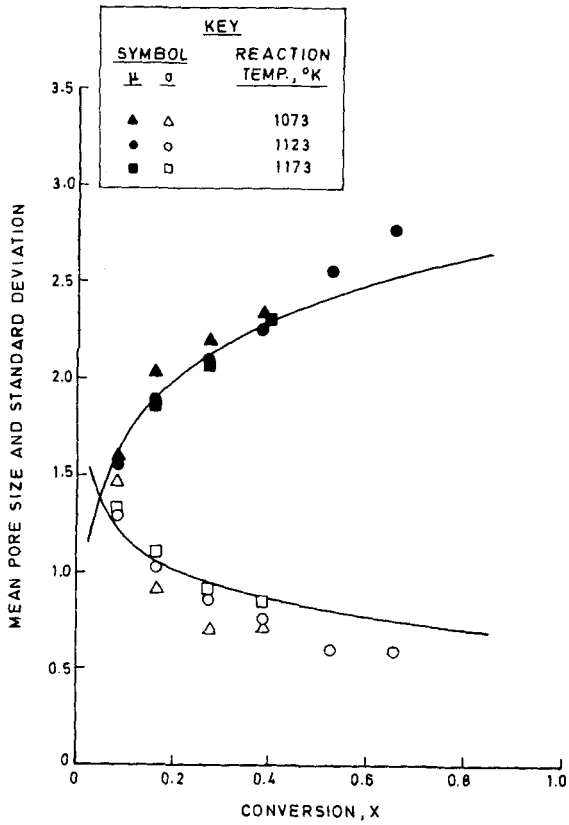

Figure 7. Effect of conversion on mean pore size and standard deviation, assuming a log-normal distribution of pore sizes. Experimental data are from Kawahata and Walker (1962).

dictions of Eq. 28, even though the reaction might be expected to exhibit some pore diffusional resistance in the temperature range used in these studies. The model calculations were based on initial porosity $\epsilon_0 = 0.113$, which again was obtained from the total pore volumes reported at zero and 65% conversion.

Although the pore size distribution of this Anthracite char is narrow enough to be modeled as a single pore size, Kawahata and Walker also offered an alternative approach. They approximated the pore volumes over the pore diameter range from 3 to 30 Å by a log-normal distribution:

$$v(r) = \frac{1}{\sqrt{2\pi}\sigma\,(2r)} \exp\left[-\frac{(ln\,2r - \mu)}{2\sigma^2}\right] \qquad (43)$$

where μ and σ are the mean and standard deviation, respectively.

Kawahata and Walker estimated means and standard deviations from the experimental measurements at different burn-offs. For comparison with the data-generated means and standard deviations, these parameters were also obtained from distributions calculated via Eqs. 4 and 40 starting from an initial log-normal shape, even though it is understood that the shape of the distribution must change with conversion since the small pores grow faster than the large.

For example, the reported μ and σ at 8% burn-off are given as 1.52 and 1.30, respectively, corresponding to a log-normal distribution with 95% of all pore volume contained within the approximate range $-1.0 \le ln(2r) \le 4.0$. At 21% conversion, although the computed distribution is no longer a log-normal curve, this pore size range would evolve to $-0.02 \le ln(2r) \le 4.00$, corresponding to $\mu = 1.99$ and $\sigma = 1.00$ in a log-normal fit if 95% of the pore volume were within this range. The results shown in Figure 7 compare the experimental and computed values obtained in this fashion, supporting the proposed technique based on Eqs. 40 and 4. It should be noted that the calculation was based on the fit at 8% conversion, since the μ and σ of the initial pore structure were not provided in the reference paper.

The development of this work can be useful for designing or tailoring the pore structure of activated carbons for specific uses. Some activated carbons are intended for example to be used as molecular sieves to selectively adsorb only certain molecules (Walker et al., 1966). Such capability is closely associated with the amount of pore volume contained in pores of certain sizes, and as a result too much or too little pore size enlargement may result in a loss of this ability to discriminate by adsorption. For a material with a given initial pore structure, Eqs. 40 and 4 can be used to determine an optimal reaction time or conversion level for maximum pore volume within the desired size ranges. Similarly, they can also be used to select initial pore structures that are most appropriate for activation. Finally, it should be noted in justification of the assumptions made above that carbon activations are typically endothermic reactions operated in or near the regime of chemical kinetic control.

ACKNOWLEDGMENT

This research was funded by the U.S. Department of Energy Fossil Research Program under Contract No. EX 76-S-01-2450.

NOTATION

a,b = stoichiometric coefficients
A = gas reactant
B = solid reactant
C = concentration of gas reactant
$f(r,t)$ = length distribution of nonoverlapped system at any time t
G = quantity defined by Eq. 2
k_s = rate constant for surface reaction
L_E = total pore length of a nonoverlapped system
L_{E0} = L_E at $t = 0$
r = pore radius
r_0 = initial pore radius
r_1 = small pore size in a solid with bimodal pore size distribution
r_2 = large pore size in a solid with bimodal pore size distribution
r_{10} = r_1 at $t = 0$
r_{20} = r_2 at $t = 0$
R = reaction rate per unit surface area
S = actual surface area per unit volume
S_0 = S at $t = 0$
S_E = surface area of nonoverlapped system, per unit volume
S_{E0} = S_E at $t = 0$
t = reaction time
$v(r,t)$ = actual pore volume distribution at time t
$v_E(r,t)$ = pore volume distribution of a non-overlapped system at time t
V = actual total pore volume per unit volume of space, equivalent to porosity
V_0 = V at $t = 0$
V_1 = pore volume within small size pores in a solid with biomodal pore size distribution
V_2 = pore volume within large size pores in a solid with bimodal pore size distribution
V_{10} = V_1 at $t = 0$
V_{20} = V_2 at $t = 0$
V_E = total pore volume of a nonoverlapped system, per unit volume of space
V_{E0} = V_E at $t = 0$
X = conversion

Greek Letters

ϵ_0 = initial porosity
ψ = pore structure parameter defined by Eq. (5)

LITERATURE CITED

Avrami, M., "Kinetics of Phase Change. II: Transformation-Time Relations for Random Distribution of Nuclei," *J. Chem. Phys.*, **8**, 212 (1940).

Bhatia, S. K., and D. D. Perlmutter, "A Random Pore Model for Fluid-Solid Reactions. I: Isothermal, Kinetic Control," *AIChE J.*, **26**, 379 (1980).

Cameron, A., and W. O. Stacy, "Changes in the Pore Structure of Coke during Carbonization and Gasification," *Austr, J. Appl. Sci.*, **9**, 283 (1958).

Cameron, A., and W. O. Stacy, "The Pore Structure of Chars and Cokes," *ibid*, **10**, 449 (1959).

Dutta, S., C. Y. Wen, and R. J. Belt, "Reactivity of Coal and Char. 1. In Carbon Dioxide Atmospheres," *Ind. Eng. Chem. Process Design Develop.*, **16**, No. 1, 20 (1977).

Dutta, S., C. Y. Wen, "Reactivity of Coal and Char. 2. In Oxygen-Nitrogen Atmospheres," *ibid*, **31** (1977).

Gavalas, G. R., "A Random Capillary Model with Application to Char Gasification of Chemically Controlled Rates," *AIChE J.*, **26**, 577 (1980).

Hashimoto, K., and P. L. Silveston, "Gasification: Part I. Isothermal Kinetic Control Model for a Solid With a Pore Size Distribution," *AIChE J.*, **19**, 259 (1973).

Hashimoto, K., K. Miura, F. Yoshikawa, and I. Imai, "Change in Pore Structure of Carbonaceous Materials During Activation and Adsorption Performance of Activated Carbon," *Ind. Eng. Chem. Process Design & Dev.*, **18**, 73 (1979).

Kawahata, M., and P. L. Walker, Jr., "Mode of Porosity Development in Activated Anthracite," *Proc. of the 5th Carbon Conf.*, **2**, 251, Pergamon Press, New York (1962).

Lamond, T. G., and H. Marsh, "The Surface Properties of Carbon. II: The Effect of Capillary Condensation at Low Relative Pressures upon the Determination of Surface Area," *Carbon*, **1**, 293 (1964).

Patel, R. L., S. P. Nandi, and P. L. Walker, Jr., "Molecular Sieve Characteristics of Slightly Activated Anthracite," *Fuel*, **51**, 47 (1972).

Petersen, E. E., "Reaction of Porous Solids," *AIChE J.*, **3**, 442 (1957).

Simons, G. A., and M. L. Finson, "The Structure of Coal Char: Part I: Pore Branching," *Comb. Sci. Tech.*, **19**, 217 (1979).

Simons, G. A., "The Structure of Coal Char. II: Pore Combination," *ibid.*, **19**, 227 (1979).

Szekely, J., J. W. Evans, and H. Y. Sohn, *Gas-Solid Reactions*, Academic Press, London (1976).

Tomkow, K., A. Jankowska, F., Czechowski, and T. Siemieniewska, "Activation of Brown-Coal Chars with Oxygen," *Fuel*, **56**, 101 (1977).

Walker, Jr., P. L., L. G. Austin, and S. P. Nandi, "Activated Diffusion of Gases in Molecular-Sieve Materials," *Chem. and Phys. of Carbon*, **2**, 257, Marcel Dekker, New York (1966).

Walker, Jr., P. L., "Pore System in Coal Chars: Implications for Diffusion Parameters and Gasification," *Fuel*, **59**, 809 (1980).

Manuscript received April 27, 1983; revision received September 22, and accepted September 30, 1983.